Proceedings (CD) of the 3rd International Conference on Porous Media and its Applications in Science and Engineering
ICPM3
June 20-25, 2010, Montecatini, Italy

Effects of Fiber Orientation on Flow Properties of Fibrous Porous Structures at Moderate Reynolds Number

A. Tamayol, K.W. Wong, M. Bahrami
Mechatronic System Engineering
School of Engineering Sciences
Simon Fraser University, BC, Canada
ali_tamayol@sfu.ca

Abstract

In this study, effects of porosity and fiber orientation on the viscous permeability and Forchheimer coefficient of mono-dispersed fibers are investigated. The porous material is represented by a unit cell which is assumed to be repeated throughout the medium. Based on the orientation of the fibers in the space, fibrous media are divided into three categories: 1D, 2D, and 3D structures. Parallel and transverse flow through square arrangements of 1D fibers, simple 2D mats, and 3D simple cubic structures are solved numerically over a wide range of porosities, 0.35 < ε < 0.95 and Reynolds numbers 0.01 < Re < 200. The results are used to calculate permeability and the inertial coefficient of the solid matrices. An experimental study is performed; the flow coefficients of three different ordered tube banks in the moderate range of Reynolds number, 0.001 < Re < 15, are determined. The numerical results are successfully compared with the present and the existing experimental data in the literature. The results suggest that permeability and Forchheimer coefficient are functions of porosity and fiber orientation. A comparison of the experimental and numerical results with Ergun equation reveals that this equation is not suitable for highly porous materials. As such, new, accurate correlations are proposed for determining the Forchheimer coefficient in fibrous media.

Keywords: Fibrous media; Flow coefficients; Inertial regime; Numerical modeling; Experimental;

1 Introduction

In-depth understanding of flow through fibrous porous materials and determining the resulting pressure drop are important in numerous engineering applications such as filtration and separation of particles [1], biological systems [2], composite fabrication [3], compact heat exchangers [4,5], and fuel cell technology [6]. In creeping flow regime, according to Darcy equation the relationship between volume averaged velocity through porous media, U_D, and the pressure drop is linear [7]:

$$-\frac{dP}{dx}=\frac{\mu}{K}U_D \tag{1}$$

where K is the permeability. In higher Reynolds numbers, the relationship becomes parabolic and a modified Darcy equation can be used [7]:

$$-\frac{dP}{dx}=\frac{\mu}{K}U_D+\beta U_D^2 \tag{2}$$

where β is called the inertial coefficient. For a fibrous medium, the flow coefficients are expected to depend on the porosity, fibers diameter, fibers distribution in the volume, and the orientation of fibers relative to the flow direction.

Based on the orientation of the fibers in space, three categories can be considered for fibrous structures: one-directional (1D) where the axes of fibers are parallel to each other; two-directional (2D) where the fibers axes are located on planes parallel to each other, with an arbitrary distribution and orientation on these planes; and three-directional (3D), where their axes are randomly positioned and oriented in a given volume. With the exception of the 3D structures, the rest are not isotropic [8].

A variety of analytical, theoretical, and experimental methods have been employed to predict the flow properties of fibrous materials. Existing analytical works are mostly limited to study of the creeping flow over a single cylinder or through periodic fiber arrays [9-16]. In addition, few models have been reported that are capable of predicting the permeability of 2D and 3D structures [1,17-20]; recently, Tamayol and Bahrami [20] have reviewed these models. Numerical and experimental studies for creeping flow in fibrous media covers a wider range of porosity and fiber distribution in 1D [19, 21-22], 2D [19,23-27], and 3D [28-31] structures. Most of the existing correlations in literature for 2D and 3D are based on curve fitting of numerical and experimental data [8].

Considering the inertial effects in the flow analysis adds to the complexity of the problem. As such, no analytical solutions were found in the literature for the moderate Reynolds number flows through fibrous structures. The existing studies are either numerical or experimental. Effects of Reynolds number on the pressure drop through unidirectional mono-disperse and bimodal fibers were investigated numerically by Nagelhout et al. [32], Martin et al. [33], Lee and Yang [34], Koch and Lodd [35], Edwards et al. [36], Ghaddar [37] and Papathanasiou et al. [38]. Their results, in general, confirmed a parabolic relationship between pressure drop and flow rate in the considered geometries. However, comparison of these numerical results with conventional models in the literature such as the Ergun equation was not successful [38].

The studies of moderate Reynolds number flows through 2D and 3D structures are not frequent. Recently, Rong et al. [39] used Lattice Boltzmann method to investigate the flow in three dimensional random fiber network with porosities in the range of $0.48 < \varepsilon < 0.72$. Their results were in agreement with Forchheimer equation which is in line with the observations of [38]. Boomsma et al. [40] have also studied flow in high porosity 3D fibrous structures to predict flow properties of open cell aluminum foams.

Our literature review reveals that no comprehensive studies exists in the literature on the effect of microstructure especially fiber orientation on the flow properties of fibrous materials in low to moderate range of Reynolds numbers. In addition, very few experimental works have been published for the flow through ordered fibrous with moderate Reynolds number. In this study, the effects of porosity and fiber orientation on the flow coefficients of mono-dispersed fibers are investigated. Parallel and transverse flow through a variety of fibrous matrices including square fiber arrangements, simple two directional mats, and simple cubic structures are solved numerically over a wide range of porosities, $0.4 < \varepsilon < 0.95$ and Reynolds numbers $0.01 < Re < 200$. The results are then used to find permeability and the inertial coefficient of the solid matrices. To verify the present numerical results, pressure drop through three different tube banks with porosity range of $0.8 < \varepsilon < 0.9$ are tested using water-glycerol mixtures to determine the flow coefficients. The numerical results are successfully compared with the present experimental measurements and the data found in the literature. The results showed that both permeability and inertial coefficient are functions of porosity and fiber orientation. However, the dependence on the fibers orientation is more pronounced in lower porosities, i.e., $\varepsilon < 0.7$. Moreover, using the present numerical results, new compact correlations are proposed for calculating the inertial coefficient in the considered structures.

2 Geometrical modeling

Following other researchers [17-20, 32-38], the porous media is represented by a unit cell which is assumed to be repeated throughout the media. The flow properties of square arrays of equally-sized, equally-spaced fibers, shown in Fig. 1, are studied as a representative of 1D structures. The solid volume fraction, φ, for the arrangement shown in Fig. 1 is related to the distance between the centers of adjacent fibers, S, and the fibers diameter, d:

$$\varphi = \frac{\pi d^2}{4S^2} \tag{3}$$

To model 2D woven textile materials, the geometry shown in Fig. 2 is considered. The relationship between solid volume fraction φ and other geometrical parameters in Fig. 2 can be expressed as:

$$\varphi = \frac{\pi d}{4S} \tag{4}$$

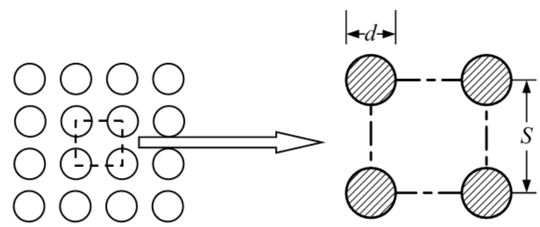

Figure 1: Square fiber arrangement for analysis of 1D structures.

The flow properties of SC structures are investigated as a representative structure for 3D materials; see Fig. 3. The relationship between the solid volume fraction and geometric parameters of SC arrangement is [30]:

$$\varphi = \frac{3\pi d^2}{4S^2} - \sqrt{2}\frac{d^3}{S^3} \tag{5}$$

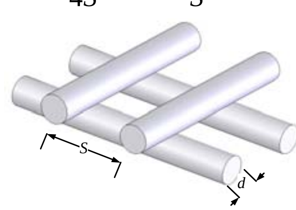

Figure 2: Considered unit cells for modeling 2D fibrous structures.

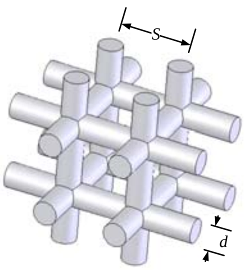

Figure 3: Simple cubic unit cells for modeling 3D structures.

3 Microscopic and macroscopic flow equations

If the pore sizes are much larger than the molecular mean free path, flow in pore scale is governed by Navier-Stokes equation; that is the continuum flow hypothesis which is considered here. Assuming incompressible, steady state flow, the microscopic equations become [7]:

$$\nabla . \vec{u} = 0 \tag{6}$$

$$\rho \vec{u} . \nabla \vec{u} = -\nabla P + \mu \nabla^2 \vec{u} \tag{7}$$

where $\vec{u}$ is the pore scale velocity vector, ρ and μ are the fluid density and viscosity, respectively . After volume averaging, Eq. (7) leads to Eq. (2) and in creeping flow limit, reduces to Eq. (1). Equation (2) is usually written in the following form [7]:

$$-\nabla P = \frac{\mu}{K} U_D + \frac{\rho F}{\sqrt{K}} U_D^2 \tag{8}$$

where F is a dimensionless number called Forchheimer coefficient. An especial form of Eq. (6) is the Ergun equation:

$$-\nabla P = 150 \frac{(1-\varepsilon)^2}{\varepsilon^3 d^2} U_D + 1.75 \frac{(1-\varepsilon)}{\varepsilon^3 d} U_D^2 \tag{9}$$

where $K = \varepsilon^3 d^2 / 150(1-\varepsilon)^2$ and $F = 0.14 / \varepsilon^{3/2}$. Ergun equation is based on a curve fit of experimental data collected for granular materials [7].

4 Experimental approach

The permeability and inertial coefficient of three different 1D tube banks with square arrangement were measured. Several water-glycerol mixtures with different mass concentrations were used to change the flow Reynolds number from 0.001 to 15. The properties and the measured coefficient of the tested samples are summarized in Table 1.

A gravity driven test bed was custom-built. The test apparatus consisted of an elevated reservoir, an entry section, sample holder, and an exit section with a ball valve as schematically shown in Fig. 4. To test different samples, tube banks were interchangeable and could be inserted into the sample holder. The liquid level in the elevated reservoir tank was kept constant during the experiment to ensure a constant pressure head. The pressure drop across the samples was measured using a differential pressure transducer, PX-154 BEC Controls with %1 accuracy. To minimize entrance and exit effects on the pressure drop measurements, pressure taps were located far from the first and the last tube rows in the tube bank samples. The bulk flow was calculated using a precision scale by weighting the collected test fluid over a set period of time.

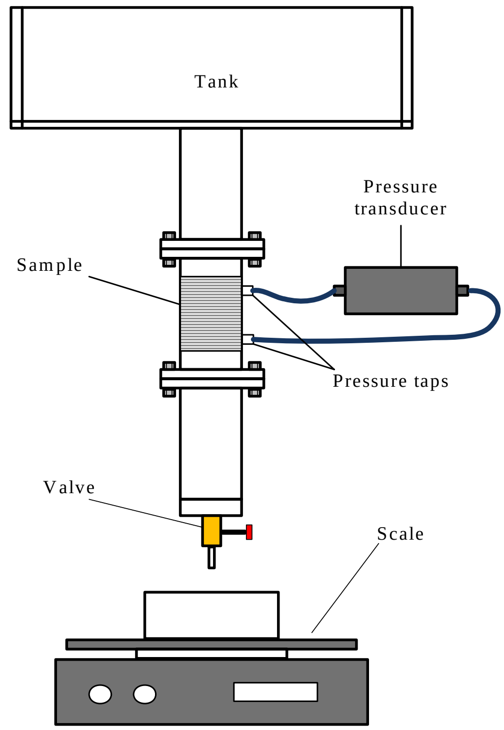

Figure 4: Schematic of the test setup.

To obtain the permeability and the inertial coefficient from the measured pressure drop (dp/dx) and mass flow values, the volume averaged superficial velocity, U_D, was calculated from the mass flow rate data and then $1/\mu U_D \left(dp/dx\right)$ was plotted versus $\rho U_D / \mu$. The y-intercept and the slope of the data were then $1/K$ and $F/\sqrt{K}$, respectively; see Eq. (8). Using equation (2), the inertial coefficient was found. From Fig.5, it can be seen that the measured pressure drops present a parabolic relationship with the volume-averaged velocity.

5 Numerical procedure

Equations (6) and (7) are solved using Fluent [42] which is a finite volume based software. The second order upwind scheme is selected to discretize the governing equations and SIMPLE algorithm [42] is employed for pressure-velocity coupling. The inlet and outlet boundaries of the computational domains are considered to be periodic. The symmetry boundary condition is applied on the side borders of the considered unit cells; this means that normal velocity and gradient of parallel component of the velocity on the side borders are zero. Structured grids and unstructured grids are generated for 1D/2D and 3D networks, respectively, using Gambit [41], the preprocessor in Fluent package.

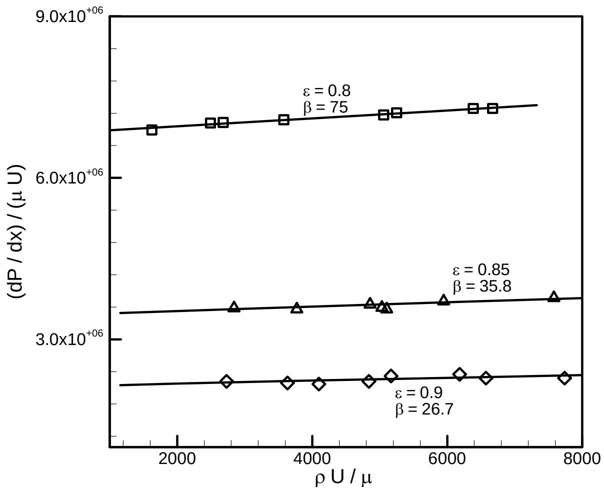

Figure 5: Measured values of $1/\mu U_D \left(dp/dx\right)$ for the samples of tube bank with square fiber arrangement.

Numerical grid aspect ratios are kept in the range of 1-5. Grid independence is tested for different cases and the size of the computational grids used for each geometry is selected such that the maximum difference in the predicted values for pressure gradient be less than 2%. The maximum number of grids used for 1D structures and 2D/3D are approximately 14k and 1400k, respectively. It should be noted that the convergence criterion, maximum relative error in the value of dependent variables between two successive iterations, is set at 10^{-6}.

In the present study, numerical simulations are carried out for fibrous networks in the porosity range of 0.3 - 0.95 and in the Reynolds number range of 0.001 – 200. With the exception of SC structures the other considered unit cells are anisotropic [8]; therefore, numerical simulations are conducted for flow parallel to different coordinate axes. The same method as described in the previous part is employed to determine the permeability and the inertial/Forchheimer coefficient from numerical results for different unit cells. The summary of the computed flow coefficients are reported in Table 2.

Flow parallel to axes of square arrays of cylinders is similar to laminar channel flows. This leads to zero value for Forchheimer coefficient in parallel flow as reported in Table 1. Similarly, for 2D structures, the in-plane Forchheimer coefficients have lower values than the calculated values for through-plane flow. This is resulted from the fact that 50% of the fibers in the considered geometry are parallel to the flow for the case. Therefore, no inertial drag forces are exerted on these fibers.

6 Comparison of the numerical results with existing data in the literature

6.1 Square arrangement (1D)

To verify the numerical analysis, in Fig. 6 the calculated values of the dimensionless normal permeability, K/d^2, are successfully compared with present experimental results and the data collected from several sources [43-48]. In addition, in Fig. 7 the calculated Forchheimer coefficients for square arrangements are compared with the present experimental data, the numerical results of Ghaddar [37] and Papatanasiou et al. [38] for monodisperse and bimodal fiber arrays, respectively. In addition, the experimental data of Berglin et al. [48] (oil flowing across tube banks) are included in Fig. 8. In general, the present results capture the trend and are in good agreement with the collected and reported data by others.

6.2 2D and 3D simple cubic structures

To the best knowledge of the authors, there are no experimental data for moderate Reynolds flow through the considered 2D and 3D structures in the open literature. To verify our analysis, in Fig. 8 the calculated permeability values for simple cubic arrangement are successfully compared with the numerical results of Higdon and Ford [30] and experimental data for actual 3D materials collected from different sources. The plotted data are based on permeability results for polymer chain in solutions [49], glass wool randomly packed, stainless steel crimps [20, 50], metallic fibers [51], and aluminum metal foams [27,52].

Table 1: Summary of the properties of the tested samples; water-glycol used as test fluid.

Sample type	ε	d (mm)	Orientation	$K\,(m^2)$	$\beta\,(m^{-1})$	F
Tube bank (square)	0.8	1.5	1D	1.38×10^{-7}	75	0.028
Tube bank (square)	0.85	1.5	1D	3.74×10^{-7}	35.8	0.022
Tube bank (square)	0.9	1.5	1D	5.44×10^{-7}	26.7	0.020

Table 2: Flow properties for the considered fibrous structures.

Square array (1D)					
Normal flow			Parallel flow		
ε	K/d^2	F	ε	K/d^2	F
0.45	0.0015	0.189	0.45	0.0079	0
0.65	0.014	0.032	0.55	0.0177	0
0.8	0.072	0.020	0.65	0.0378	0
0.9	0.300	0.011	0.8	0.1667	0
0.95	0.892	0.010	0.9	0.643	0
Planar structures (2D)					
Through plane flow			In-plane flow		
ε	K/d^2	F	ε	K/d^2	F
0.35	0.0007	0.313	0.35	0.0016	0.092
0.5	0.0046	0.118	0.5	0.0069	0.046
0.6	0.012	0.091	0.6	0.0164	0.033
0.8	0.106	0.033	0.8	0.0807	0.018
0.9	0.439	0.0028	0.9	0.4119	0.013
Simple cubic (3D)					
ε	K/d^2	F			
0.31	0.0011	0.914			
0.37	0.0023	0.562			
0.59	0.0174	0.141			
0.79	0.118	0.041			
0.87	0.336	0.024			

7 Effects of fiber orientation on flow properties

Effects of microstructure and more specifically fibers orientation on permeability and Forchheimer coefficient are investigated in Figs. 9 and 10, respectively. As expected, 1D arrangements are the most anisotropic geometry and the normal and parallel permeability of such structures provide the lower and upper bounds for permeability of fibrous media. Effects of microstructure are more pronounced in lower porosities.

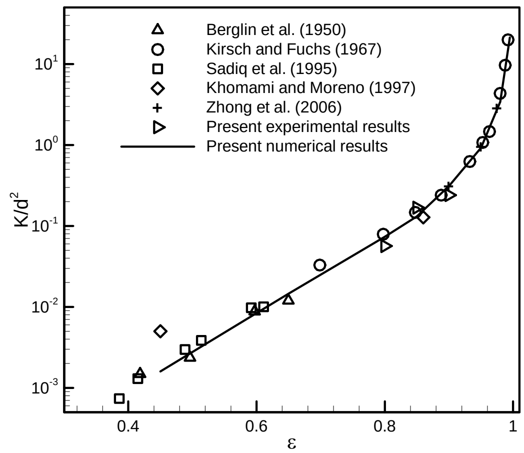

Figure 6: Comparison between the present numerical results, collected experimental results, and data from various sources, for normal flow through square fiber arrays.

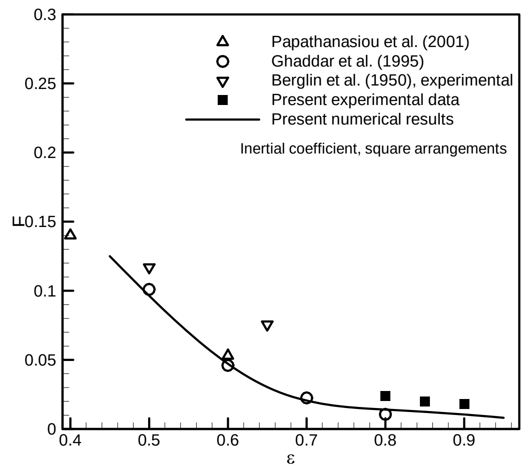

Figure 7: Comparison between the present numerical and experimental results for Forchheimer coefficient with experimental and numerical data of others.

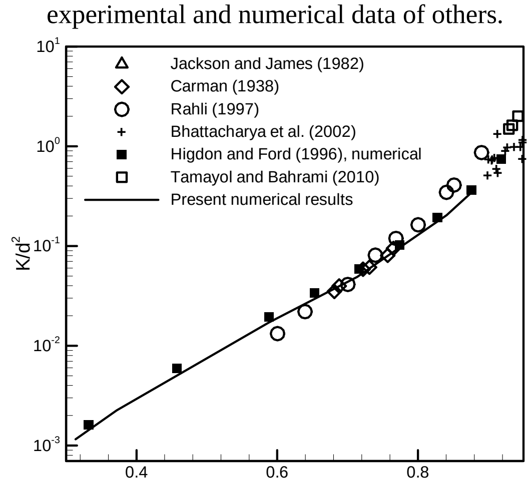

Figure 8: Comparison between the present numerical results for permeability of simple cubic arrangements with existing numerical and experimental data of 3D materials.

The plotted data in Fig. 9 indicates that 1D and 2D geometries are anisotropic and the Forchheimer coefficient for 3D structures is higher than values for 1D and 2D geometries. The Forchheimer coefficient is a reflection of inertial effects. Thus, it is more influenced by microstrucutre in lower porosities, i.e., $\varepsilon < 0.7$.

8 Comparison with the Ergun equation

Ergun equation, Eq. (9), is a widely accepted equation for prediction of pressure drop across granular materials. Two main differences between fibrous and granular materials are:

1) Shape of the particles in granular materials are spherical while fibrous media are made up of cylindrical like particles.
2) Porosity of granular materials are in the range of 0.2 – 0.6, where fibrous materials usually have higher porosities, $0.6 < \varepsilon < 0.999$.

The present numerical results are compared with the values predicted by the Ergun equation to figure out if this equation is applicable to high porosity fibrous structures. Figure 9 includes the predicted values of permeability from Ergun equation and present numerical results. It can be seen that the Ergun equation can only predict trends of numerical data qualitatively and the differences are significant especially in low porosities. The Forchheimer results calculated from the Ergun equation are plotted against the current numerical results in Fig. 10. The comparison shows that the Ergun equation is only in agreement with numerical results for isotropic 3D materials with low porosities. For higher porosities Eq. (9) is incapable of predicting pressure drop for fibrous media.

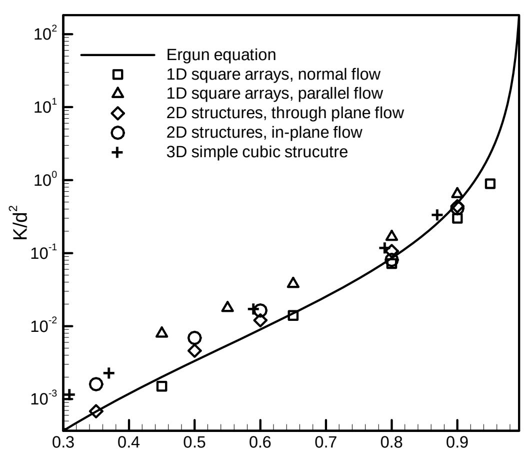

Figure 9: Comparison of numerical values of dimensionless permeability of fibrous media with Ergun equation.

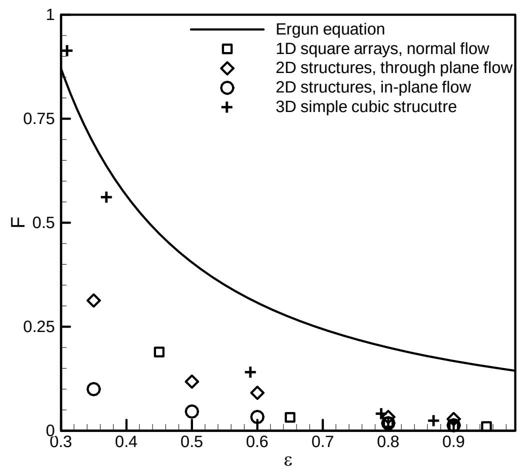

Figure 10: Comparison of numerical values of Forchheimer coefficient of fibrous media with Ergun equation.

8 Correlations for Forchheimer coefficient

Our analysis showed that the Ergun equation is not accurate for prediction of the permeability and the Forchheimer coefficient of fibrous porous materials. Creeping flow through fibrous media has been investigated by various research groups and several models exist for calculating the permeability. However, only few studies have been performed to investigate the inertial flow regime in fibrous porous media.

Using our numerical results, a series of compact correlations are developed for 1D, 2D, and 3D fibrous structures and are listed in Table 3. The proposed correlations are accurate within 2% of the present numerical results.

Table 3: Proposed correlations for Forchheimer coefficient in fibrous media.

Flow direction/microstructure	$F=\left(a+b\,\varepsilon\right)^{-1/c}$		
	a	b	c
Normal/square arrays (1D)	-3.491	12.51	0.456
Through plane- 2D structures	-0.14	5.05	0.418
In-plane/2D structures	1.037	0.0863	0.025
Simple cubic arrangements (3D)	0.534	1.56	0.184

9 Conclusions

The effects of porosity and fiber orientation on the viscous permeability and the Forchheimer coefficient of mono-dispersed fibers were investigated. Fibrous porous materials were classified into three main categories: 1D, 2D, and 3D structures. Using a unit-cell approach, the flow through the considered geometries (1D, 2D, and 3D) were solved numerically over a wide range of Reynolds number, $0.01 < \mathrm{Re} < 200$. The results were then used to calculate permeability and the inertial coefficient of the solid matrices.

An experimental study was undertaken. The permeability and the inertial coefficient in three samples of 1D tube banks with square arrangement were measured over a range of the Reynolds number. The present numerically computed permeabilities were successfully compared with the present experimental results and the data collected from various sources. The results suggested that both permeability and Forchheimer coefficients were functions of porosity and fiber orientation. In addition, a comparison of the numerical results with Ergun equation reveals that this equation was not accurate for highly porous materials. From the numerical study, new compact accurate correlations were proposed for determining the Forchheimer coefficient in fibrous media.

10 Acknowledgments

The authors gratefully acknowledge the financial support of the Natural Sciences and Engineering Research Council of Canada, NSERC.

11 References

[1] L. Spielman, S.L. Goren, 1968, "Model for predicting pressure drop and filtration efficiency in fibrous media," Current Research, Vol. 2, pp. 279-287.

[2] G.A. Truskey, F. Yuan, D.E. Katz, 2004 "Transport phenomena in biological systems," Pearson Prentience Hall, New Jerseys.

[3] B.T. Astrom, R.B. Pipes, S.G. Advani, 1992, "On flow through aligned fiber beds and its application to composite processing," Journal of Composite Materials, Vol. 26 (9), pp. 1351-1373.

[4] L. Tadrist, M. Miscevic, O. Rahli, F. Topin, 2004, "About the use of fibrous materials in compact heat exchangers," Experimental Thermal and Fluid Science, Vol. 28, pp. 193–199.

[5] S. Mahjoob, K. Vafai, 2008, "A Synthesis of Fluid and Thermal Transport Models for Metal Foam Heat Exchangers," International Journal of Heat and Mass Transfer, Vol. 51, pp. 3701–3711.

[6] J.T. Gostick, M.W. Fowler, M.D. Pritzker, M.A. Ioannidis, L.M. Behra, 2006, "In-plane and through-plane gas permeability of carbon fiber electrode backing layers," Journal of Power Sources, Vol. 162, pp. 228-238.

[7] M. Kaviany, 1992, "Principles of heat transfer in porous media," Springer-Verlag, New York.

[8] M.M. Tomadakis, T. Robertson, 2005, "Viscous permeability of random fiber structures: comparison of electrical and diffusion estimates with experimental and analytical results," Journal of Composite Materials, Vol. 39, pp. 163-188.

[9] J. Happel, 1959, "Viscous flow relative to arrays of cylinders," AICHE, Vol. 5, pp. 174–177.

[10] S. Kuwabara, 1959, "The forces experienced by randomly distributed parallel circular cylinders or spheres in a viscous flow at small Reynolds numbers," Journal of Physical Society of Japan, Vol. 14, pp. 527-532.

[11] H. Hasimoto, 1959, "On the periodic fundamental solutions of the stokes equations and their application to viscous flow past a cubic array of spheres," Journal of Fluid Mechanics, Vol. 5, pp.317–328.

[12] A.S. Sangani, A. Acrivos, 1982, "Slow flow past periodic arrays of cylinders with application to heat transfer," International Journal of Multiphase Flow, Vol. 8, pp.193–206.

[13] J.E. Drummond, M.I. Tahir, 1984, "Laminar viscous flow through regular arrays of parallel solid cylinders," International Journal of Multiphase Flow, Vol. 10, pp. 515-540.

[14] E.M. Sparrow, A.L. Loeffler, 1959, "Longitudinal Laminar Flow between Cylinders Arranged in Regular Array," AICHE, Vol. 5, pp. 325-330.

[15] B.R. Gebart, 1992, "Permeability of Unidirectional Reinforcements for RTM," Journal of Composite Materials, Vol. 26, pp. 1100-1133.

[16] A. Tamayol, and M. Bahrami, 2009, "Analytical determination of viscous permeability of fibrous porous media," International Journal of Heat and Mass Transfer, Vol. 52, pp. 3691-3701.

[17] M.M. Tomadakis, S.V. Sotirchos, 1993, "Transport properties of random arrays of freely overlapping cylinders with various orientation distributions," Journal of Chemical Physics, Vol. 98, pp. 616–626.

[18] G.W. Jackson, D.F. James, 1986, "The permeability of fibrous porous media," Canadian Journal of Chemical Engineering, Vol. 64, pp. 364–374.

[19] M.P. Sobera, and C.R. Kleijn, 2006, "Hydraulic permeability of ordered and disordered single-layer arrays of cylinders," Physical Review E, Vol. 74, pp. 036302-1-10.

[20] A. Tamayol, and M. Bahrami, 2010, "Transverse Permeability of Fibrous Porous Media," 3nd International Conference on Porous Media and its Applications in Science and Engineering, Montecatini, Italy.

[21] M. Sahraoui, M. Kaviany, 1994, "Slip and no-slip boundary condition at interface of porous, plain media," International Journal of Heat and Mass Transfer, Vol. 37, pp. 1029–1044.

[22] A.S. Sangani, C. Yao, 1988, "Transport processes in random arrays of cylinders: II-viscous flow," Physics of Fluids, Vol. 31, pp. 2435-2444.

[23] S. Jaganathan, H. Vahedi Tafreshi, , B. Pourdeyhimi, 2008, "On the Pressure Drop Prediction of Filter Media Composed of Fibers With Bimodal Diameter Distributions," Powder Technology, Vol. 181, pp. 89–95.

[24] S. Jaganathan, H. Vahedi Tafreshi, , B. Pourdeyhimi, 2008, "A Realistic Approach for Modeling Permeability of Fibrous Media: 3-D Imaging Coupled with CFD Simulation," Chemical Engineering Science, Vol. 63, pp. 244 – 252.

[25] A. Koponen, D. Kandhai, E. Hellén, M. Alava, A. Hoekstra, M. Kataja, K. Niskanen, P. Sloot, J. Timonen1, 1998, “Permeability of Three-Dimensional Random Fiber Webs,” Physical Review Letters, Vol. 80, pp. 716-719.

[26] L. Hao, P. Cheng, 2009, “Lattice Boltzmann simulations of anisotropic permeabilities in carbon paper gas diffusion layers,” Journal of Power Sources, Vol. 186, pp. 104–114.

[27] M.A. Van Doormaal, J.G. Pharoah, 2009, “Determination of permeability in fibrous porous media using the lattice Boltzmann method with application to PEM fuel cells,” International Journal of Numerical Methods for Fluids, Vol. 59, pp. 75–89.

[28] M. Palassini, A. Remuzzi, 1998, “Numerical analysis of viscous flow through fibrous media: a model for glomerular basement membrane permeability,” American Journal of Physiology-Renal Physiology, Vol. 274, pp. 223-231.

[29] D.S. Clauge, B.D. Kandhai, R. Zhang, and P.M.A. Sloot, 2000, “Hydraulic permeability of (un)bounded fibrous media using the lattice Boltzmann method”, Physical Review E, Vol. 61, pp. 616-625.

[30] J.J.L. Higdon, G.D. Ford, 1996, Permeability of three-dimensional models of fibrous porous media, Journal of Fluid Mechanics, Vol. 308, pp. 341-361.

[31] A. Nabovati, E.W. Llewellin, A.C.M. Sousa, 2009, “A general model for the permeability of fibrous porous media based on fluid flow simulations using the lattice Boltzmann method,” Composites: Part A, Vol. 40, pp. 860–869.

[32] D. Nagelhout, M. S. Bhat, J. C. Heinrich, and D. R. Poirier, 1995, ‘‘Permeability for flow normal to a sparse array of fibers,’’ Material Science Engineering A, Vol. 191, pp. 203 1995.

[33] A. R. Martin, C. Saltiel, and W. Shyy, 1998, ‘‘Frictional losses and convective heat transfer in sparse, periodic cylinder arrays in cross flow,’’ International Journal of Heat and Mass Transfer, Vol. 41, pp. 2383-2397.

[34] S.L. Lee, J.H. Yang, 1997, “Modeling of Darcy-Forchheimer drag for fluid flow across a bank of circular cylinders,” International Journal of Heat and Mass Transfer, Vol. 40, pp. 3149-3155.

[35] D.L. Koch, A.J.C. Ladd, 1997, “Moderate Reynolds number flows through periodic and random arrays of aligned cylinders,” Journal of Fluid Mechanics, Vol. 349, pp. 31-66.

[36] D.A. Edwards, M. Shapiro, P. Bar-Yoseph, M. Shapira, 1990, ‘‘The influence of Reynolds number upon the apparent permeability of spatially periodic arrays of cylinders,’’ Physics of Fluids, Vol. 2, pp. 45-55.

[37] C. K. Ghaddar, 1995, ‘‘On the permeability of unidirectional fibrous media: A parallel computational approach,’’ Physics of Fluids, Vol. 7, pp. 2563-2586.

[38] T. D. Papathanasiou, B. Markicevic, E. D. Dendy, 2001, “A computational evaluation of the Ergun and Forchheimer equations for fibrous porous media,” Physics of Fluids, Vol. 13, pp. 2795-2804.

[39] X. Rong, G. He, D. Qi, 2007, “Flows with Inertia in a Three-Dimensional Random Fiber Network,” Chemical Engineering Communications, Vo. 194, pp. 1–9.

[40] K. Boomsma, D. Poulikakos, Y. Ventikos, 2003 “Simulations of flow through open cell metal foams using an idealized periodic cell structure,” International Journal of Heat and Fluid Flow, Vol. 24, pp. 825–834

[41] Fluent 6.3 Users’ Guide, 2007, Fluent Inc., Lebanon, USA.

[42] H.K. Versteeg, W. Malalasekera, 1995, “An Introduction to Computational Fluid Dynamics,” Longman Scientific and Technical.

[43] O.P. Bergelin, G.A. Brown, H.L. Hull, F.W. Sullivan, 1950, “Heat transfer and fluid friction during viscous flow across banks of tubes: III – a study of tube spacing and tube size,” ASME Transactions; Vol. 72, pp. 881–888.

[44] A.A. Kirsch, N.A. Fuchs, 1967, “Studies on fibrous aerosol filters: II- pressure drops in systems of parallel cylinders,” Annals of Occupational Hygiene, Vol. 10, pp. 23–30.

[45] T.A.K. Sadiq, S.G. Advani, R.S. Parnas, 1995, “Experimental investigation of transverse flow through aligned cylinders,” International Journal of Multiphase Flow, Vol. 21, pp. 755–774.

[46] B. Khomami, L.D. Moreno, 1997, “Stability of viscoelastic flow around periodic arrays of cylinders,” Rheologica Acta, Vol. 36, pp. 367–383.

[47] L. Skartsis, B. Khomami, J.L. Kardos, 1992, “Resin flow through fiber beds during composite manufacturing processes, part II: numerical and experimental studies of Newtonian flow through ideal and actual fiber beds,” Polymer Engineering and Sciences, Vol. 32, pp. 231-239.

[48] W.H. Zhong, I.G. Currie, D.F. James, 2006, “Creeping flow through a model fibrous porous medium,” Experiments in Fluids, Vol. 40, pp. 119-126.

[49] D.F. James, G.W. Jackson, 1982, “The hydrodynamic resistance of hyaluronic acid and its contribution to tissue permeability”, Biorhelogy, Vol. 19, pp. 317-330.

[50] P.C. Carman, 1937, “The determination of the specific surface of powders, I.,” Journal of the Society of Chemical Industry, Vol. 57, pp. 225-234.

[51] O. Rahli, L. Tadrist, M. Miscevic, R. Santini, 1997, “Fluid flow through randomly packed monodisperse fibers: the Kozeny-Carman parameter analysis,” Journal of Fluids Engineering, Vol. 119, pp. 188-192.

[52] A. Bhattacharya, V.V. Calmidi, R.L. Mahajan, 2002, “Thermophysical properties of high porosity metal foams,” International Journal of Heat and Mass Transfer, Vol. 45, pp. 1017-1031.